Numerical study on stability of composite cutter bar milling system in rotating coordinate frame

Yuhuan Zhang[1], Yongsheng Ren[2], Jinfeng Zhang[3]

[1]School of Mechanical Engineering, Shandong University of Technology, Zibo, China

[2,3]College of Mechanical and Electronic Engineering, Shandong University of Science and Technology, Qingdao, China

[2]Corresponding author

E-mail: *1161462982@qq.com*, *Renys@sdust.edu.cn*, *zhangjf@sdust.edu.cn*

Abstract. This paper studies chatter stability of composite cutter bar milling system in rotating coordinate frame. Based on the structural dynamic equation and regenerative milling force model of composite cutter bar in rotating coordinate frame, the continuous distributed chatter analysis model of composite cutter bar milling system is established. The stability of milling system with a rotary symmetric dynamic cutter bar is predicted by using the semi-discrete time domain method. Influences including internal damping, external damping, symmetrical and asymmetric laminates on the stability of milling system are analyzed, and the results obtained in rotating and fixed coordinate frame are compared. It is shown that the results are consistent for symmetrical cutter bar either in the rotating coordinate frame or in the fixed coordinate frame. A new chatter instability zone appears at high rotating speeds due to material internal damping of the rotating composite cutter bar.

1 Introduction

Chatter can cause bad surface on the workpiece, which will affect accuracy and quality of the milling operations. Severely, the lathe will continue to bear dynamic alternating load and the tools will be damaged. Therefore, accurate prediction of the stability of machine tool system is an important guarantee for high-quality and high-efficiency machining[1].

Comparing with traditional materials, advanced fiber reinforced composites have a number of advantages including high modulus, excellent dampening properties, light weight and tailorability of mechanical properties. In recent years, they are getting more and more attention in the development of high speed cutting system tool bar[2-7].

Magnitude and direction of milling force vary periodically as the cutter bar rotates, and the dynamic model is described by delayed partial differential equations with periodic coefficients. These factors make milling process stability difficult to predict. For this reason, semi analytical method in frequency domain or numerical method in time domain is usually applied to the stability analysis of milling system[1]. Tlusty[8] replaced the periodic coefficients of delayed

partial differential equation with average angle of cutter teeth and direction of average cutting force to simplify the solution process. Minis and Yanushevsky[9] applied control theory and predicted the stability of the system by using Fourier analysis. Budak and Altintas[10] presented a multi-frequency solution for milling chatter analysis in frequency domain.

In frequency domain method, direction coefficients of time-varying milling force are expanded into Fourier series and truncated approximation is obtained. It has been shown that the zero-order approximation frequency domain method can obtain sufficiently accurate results of the stability analysis in most practical applications[1]. The time domain method, including semi-discrete method[11,12] and full-discrete method[13], usually replace the infinite dimensional single valued operator with the finite dimensional approximation of system state transfer matrix. Stability of the system is determined according to the corresponding eigenvalues. Time domain method uses discrete time interval and node iteration to search for the stability boundary. Although it requires more calculation time, it can obtain more accurate prediction results for time periodic or time invariant systems.

The dynamic equation of milling system with a rotating cutter bar can be expressed in fixed or rotating coordinates[14]. Direction coefficients of cutting force change with time in fixed coordinate frame, while they remain unchanged in rotating coordinate frame. The stiffness and damping matrix of asymmetric cutter bar are also time-dependent in fixed coordinate frame, then all of these bring great challenges for stability analysis. In rotating coordinate frame, cutting force coefficients, stiffness and damping matrix of the cutter bar are time-invariant, so the stability analysis is relatively simple and the errors caused by approximation can also be avoided.

At present, stability analysis of rotating cutter bar in most researches are obtained in fixed coordinate frame[15-21], and only a few are involved in rotating coordinate frame[22-23]. Eynian and Altintas[22] proposed a new prediction method for milling process with asymmetric structural dynamics in rotating coordinates. The stability of the characteristic equation of the system was investigated using the Nyquist stability criterion. Comak et al.[23] studied the milling process with asymmetric cutter in rotating coordinates. The stability lobes have significant differences due to the asymmetric of the structural dynamics of the system. Although these researches have involved rotating coordinate frame, the dynamic models in these researches are limited to simple two degree of freedom discrete system.

Based on the rotor dynamic theory of anisotropic structure, this paper presents the continuous distributed partial differential equation of composite cutter bar milling system in rotating coordinates. The motion equation is discretized by applying the Galerkin method. The stability of milling system is solved by the semi-discrete time domain method. The process stability of the milling system are investigated and compared with the stability prediction results which obtained in fixed coordinate frame. Moreover, influences of internal damping, external damping, symmetrical and asymmetric laminates are investigated.

2　Mathematical Model

2.1 Cutting Force Model in Rotating Coordinate Frame

Figure 1 shows the milling process in rotating coordinate frame. Number of the cutter teeth is N and rotational speed of the cutter bar is Ω.
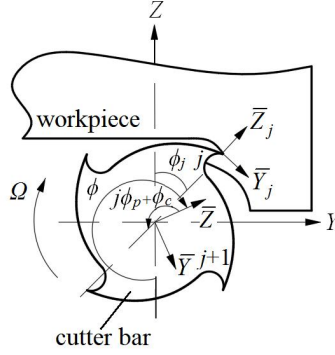

Fig. 1. Diagram of milling process in rotating coordinate frame

Dynamic chip thickness removed by tooth j is expressed in local coordinate frame $(\overline{Y}_j, \overline{Z}_j)$ as follows[23],

$$h_j(t) = c\sin\phi_j - \begin{bmatrix} 0 & 1 \end{bmatrix} \begin{Bmatrix} u_{\overline{Y}j}(t) - u_{\overline{Y}(j-1)}(t-\tau) \\ u_{\overline{Z}j}(t) - u_{\overline{Z}(j-1)}(t-\tau) \end{Bmatrix} \tag{1}$$

where c denotes the feed per revolution per tooth, ϕ_j denotes the immersion angle of tooth j, $\phi_j = \phi - j\phi_P - \phi_c$, $\phi = \Omega t$, ϕ_P denotes the pitch angle($\phi_P = 2\pi/N$), ϕ_c denotes the angle between the local rotating coordinate frame $(\overline{Y}_j, \overline{Z}_j)$ and principal rotating frame $(\overline{Y}, \overline{Z})$, and $\{u_{\overline{Y}j}(t), u_{\overline{Z}j}(t)\}$ and

$\{u_{\overline{Y}(j-1)}(t-\tau), u_{\overline{Z}(j-1)}(t-\tau)\}$ denote the vibration vectors of tooth j at time t and tooth j-1 at time $t-\tau$, respectively.

Dynamic cutting forces for tooth j can be calculated as follows,

$$\begin{Bmatrix} F_{r,j} \\ F_{t,j} \end{Bmatrix} = g(\phi_j)b\begin{pmatrix} K_r \\ K_t \end{pmatrix} h_j(t) \tag{2}$$

where K_r and K_t denote the cutting force coefficients in radial and tangential directions, b is the depth of cut, and $g(\phi_j)$ is the unit step function, where

$$g(\phi_j) = \begin{cases} 1, & \phi_{st} < \phi_j < \phi_{ex} \\ 0, & \phi_j < \phi_{st} \text{ or } \phi_j > \phi_{ex} \end{cases} \tag{3}$$

where ϕ_{st} and ϕ_{ex} are immersion angles of the cutter as it enters and leaves the cut, respectively.

Ignoring the static chip thickness $c\sin\phi_j$ and substituting Eq.(1) into Eq.(2), then the cutting force of tooth j can be obtained,

$$\left\{ \begin{matrix} F_{r,j} \\ F_{t,j} \end{matrix} \right\} = -g(\phi_j) b \left(\begin{matrix} K_r \\ K_t \end{matrix} \right) [0 \quad 1] \left\{ \begin{matrix} u_{\bar{Y}j}(t) - u_{\bar{Y}(j-1)}(t-\tau) \\ u_{\bar{Z}j}(t) - u_{\bar{Z}(j-1)}(t-\tau) \end{matrix} \right\} \qquad (4)$$

The cutting force which considered all N teeth on the cutter can be calculated as follows,

$$\left\{ \begin{matrix} F_{\bar{Y}} \\ F_{\bar{Z}} \end{matrix} \right\} = \sum_{j=0}^{N} -g(\phi_j) b T_j^{-1} \left(\begin{matrix} K_r \\ K_t \end{matrix} \right) [0 \quad 1] \left(T_j \left\{ \begin{matrix} u_{\bar{Y}}(t) \\ u_{\bar{Z}}(t) \end{matrix} \right\} - T_{j-1} \left\{ \begin{matrix} u_{\bar{Y}}(t-\tau) \\ u_{\bar{Z}}(t-\tau) \end{matrix} \right\} \right) \qquad (5)$$

where, T_j is the coordinate transformation matrix for tooth j

$$\left\{ \begin{matrix} u_{\bar{Y}j}(t) \\ u_{\bar{Z}j}(t) \end{matrix} \right\} = T_j \left\{ \begin{matrix} u_{\bar{Y}}(t) \\ u_{\bar{Z}}(t) \end{matrix} \right\} \qquad (6)$$

$$T_j = \begin{bmatrix} \cos(j\phi_p + \phi_c) & \sin(j\phi_p + \phi_c) \\ -\sin(j\phi_p + \phi_c) & \cos(j\phi_p + \phi_c) \end{bmatrix}_{2\times 2} \qquad (7)$$

2.2 The Chatter Equation of Milling System in Rotating Coordinate Frame

A tapered composite cutter bar with rotational speed Ω is shown in Figure 2, and the varying cross section radius can be expressed as: $r(X) = [1 - (1-\sigma) \cdot X/l] R_T$, where l is the length of cutter bar, $\sigma = R_R / R_T$ is the taper ratio of the cutter bar, and R_T and R_R are the external radius at the fixed and free ends, respectively.
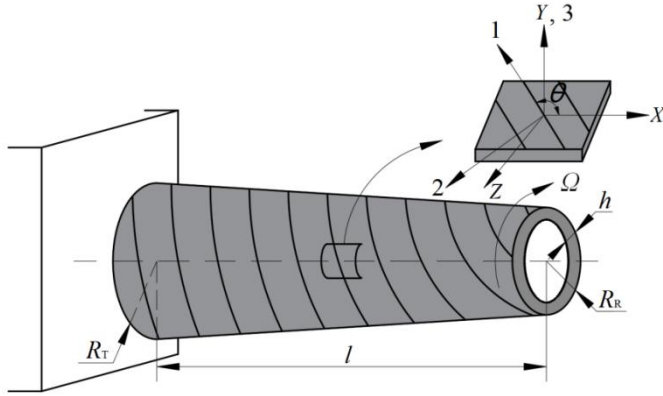

Fig. 2. Schematic diagram of the rotating tapered composite cutter bar

In fixed coordinate frame, the chatter equation of milling system with a rotating composite cutter bar obtained by Galerkin truncation can be expressed in generalized coordinates as[21]

$$M\ddot{U}(t) + C\dot{U}(t) + KU(t) = ZF(t) \qquad (8)$$

where $F(t)$ is the cutting force, M, C and K are the mass, damping and stiffness matrix of the tapered composite cutter bar respectively, where[21],

$$M = \begin{bmatrix} \overline{M}_m - \overline{I}_m & 0 \\ 0 & \overline{M}_m - \overline{I}_m \end{bmatrix},$$

$$C = \begin{bmatrix} \overline{D}^I + \overline{D}^E & -2\Omega\overline{I}_m \\ 2\Omega\overline{I}_m & \overline{D}^I + \overline{D}^E \end{bmatrix},$$

$$K = \begin{bmatrix} \overline{D} & \Omega\overline{D}^I \\ -\Omega\overline{D}^I & \overline{D} \end{bmatrix}, \tag{9}$$

$$U(t) = \begin{Bmatrix} U_{Yj}(t) \\ U_{Zj}(t) \end{Bmatrix}.$$

$$Z = \begin{bmatrix} \psi_k(l)\psi_f(l) \end{bmatrix} \quad k,f = 1,2,\cdots,S$$

$$\int_0^l m(X) \cdot \psi_i(X)\psi_j(X)\mathrm{d}X = \overline{M}_{mij},$$

$$\int_0^l I_m(X) \cdot \psi_i(X)\psi_j''(X)\mathrm{d}X = \overline{I}_{mij},$$

$$\int_0^l D_{11}(X) \cdot \psi_i''(X)\psi_j''(X)\mathrm{d}X = \overline{D}_{ij}, \tag{10}$$

$$\int_0^l c_I I(X) \cdot \psi_i''(X)\psi_j''(X)\mathrm{d}X = \overline{D}_{ij}^I,$$

$$\int_0^l c_E \cdot \psi_i(X)\psi_j(X)\mathrm{d}X = \overline{D}_{ij}^E, i,j = 1,2,\cdots,S.$$

where $m(X)$ and $I_m(X)$ are the mass per unit length and the mass moment of inertia, respectively, $D_{11}(X)$ denotes the flexural stiffness of the composite cutter bar, $I(X)$ denotes the area moment of inertia, c_I denotes Kelvin-Voigt internal damping coefficient, c_E denotes viscous external damping coefficient and $\psi_j(X)$ denote the mode shapes of a uniform, non-rotating, isotropic, cantilever Euler-Bernoulli beam. The relevant calculation expressions are shown in reference[21].

The relationship between a rotating coordinate frame and a fixed coordinate frame can be expressed as follow[23]

$$U(t) = R(t)^T \overline{U}(t) \tag{11}$$

where $\overline{U}(t) = \begin{Bmatrix} \overline{U}_{\overline{Y}j}(t) & \overline{U}_{\overline{Z}j}(t) \end{Bmatrix}^T$ denote displacement vector in rotating coordinate frame and

$R(t)^T$ is the transformation matrix, where

$$R(t)^T = \begin{bmatrix} \cos\Omega t & -\sin\Omega t \\ \sin\Omega t & \cos\Omega t \end{bmatrix} \tag{12}$$

Velocity and acceleration terms can be obtained from Eq.(11) as follows,

$$\dot{U}(t) = \boldsymbol{R}(t)^T \dot{\overline{U}}(t) + \frac{\mathrm{d}}{\mathrm{d}t} \boldsymbol{R}(t)^T \overline{U}(t) \tag{13}$$

$$\ddot{U}(t) = \boldsymbol{R}(t)^T \ddot{\overline{U}}(t) + 2\frac{\mathrm{d}}{\mathrm{d}t} \boldsymbol{R}(t)^T \dot{\overline{U}}(t) + \frac{\mathrm{d}^2}{\mathrm{d}t^2} \boldsymbol{R}(t)^T \overline{U}(t) \tag{14}$$

where,

$$\frac{\mathrm{d}}{\mathrm{d}t} \boldsymbol{R}(t)^T = \Omega \begin{bmatrix} -\sin\Omega t & -\cos\Omega t \\ \cos\Omega t & -\sin\Omega t \end{bmatrix} \tag{15}$$

$$\frac{\mathrm{d}^2}{\mathrm{d}t^2} \boldsymbol{R}(t)^T = -\Omega^2 \boldsymbol{R}(t)^T \tag{16}$$

By substituting Eqs(13) and (14) into Eq.(8), and multiplying each side by $\boldsymbol{R}(t)$, and considering Eqs(15) and (16) at the same time, then the chatter equation of milling system can be represented in rotating coordinate as

$$\overline{\boldsymbol{M}}\ddot{\overline{U}}(t) + \overline{\boldsymbol{C}}\dot{\overline{U}}(t) + \overline{\boldsymbol{K}}\overline{U}(t) = \boldsymbol{R}(t)\boldsymbol{Z}\boldsymbol{F}(t) = \overline{\boldsymbol{F}}(t) \tag{17}$$

where $\overline{\boldsymbol{M}}$, $\overline{\boldsymbol{C}}$ and $\overline{\boldsymbol{K}}$ represent mass, damping and stiffness matrix in rotating coordinate frame as

$$\overline{\boldsymbol{M}} = \begin{bmatrix} \overline{\boldsymbol{M}}_m - \overline{\boldsymbol{I}}_m & \boldsymbol{0} \\ \boldsymbol{0} & \overline{\boldsymbol{M}}_m - \overline{\boldsymbol{I}}_m \end{bmatrix},$$

$$\overline{\boldsymbol{C}} = \begin{bmatrix} \overline{\boldsymbol{D}}^I + \overline{\boldsymbol{D}}^E & -2\Omega\overline{\boldsymbol{M}}_m \\ 2\Omega\overline{\boldsymbol{M}}_m & \overline{\boldsymbol{D}}^I + \overline{\boldsymbol{D}}^E \end{bmatrix}, \tag{18}$$

$$\overline{\boldsymbol{K}} = \begin{bmatrix} \overline{\boldsymbol{D}} - \Omega^2\left(\overline{\boldsymbol{M}}_m - \overline{\boldsymbol{I}}_m\right) & -\Omega\overline{\boldsymbol{D}}^E \\ \Omega\overline{\boldsymbol{D}}^E & \overline{\boldsymbol{D}} - \Omega^2\left(\overline{\boldsymbol{M}}_m - \overline{\boldsymbol{I}}_m\right) \end{bmatrix}.$$

The cutting force expressed in rotating coordinate frame as

$$\overline{\boldsymbol{F}}(t) = \boldsymbol{Z}\left\{ \sum_{j=0}^{N} -g(\phi)b\boldsymbol{T}_j^{-1}\begin{pmatrix} K_r \\ K_t \end{pmatrix}\begin{bmatrix} 0 & 1 \end{bmatrix}\left(\boldsymbol{T}_j \begin{Bmatrix} U_{\overline{Y}k}(t) \\ U_{\overline{Z}k}(t) \end{Bmatrix} - \boldsymbol{T}_{j-1}\begin{Bmatrix} U_{\overline{Y}k}(t-\tau) \\ U_{\overline{Z}k}(t-\tau) \end{Bmatrix} \right) \right\} \tag{19}$$

2.3 The Semi-discrete Time Domain Method

According to cauchy transformation, Eq(17) can be expressed as the following first-order differential equation[11]

$$\dot{q}(t) = \boldsymbol{A}q(t) + \boldsymbol{B}q(t-\tau) \tag{20}$$

where

$$q(t) = \begin{Bmatrix} U_{\bar{Y}k}(t) \\ U_{\bar{Z}k}(t) \\ \dot{U}_{\bar{Y}k}(t) \\ \dot{U}_{\bar{Z}k}(t) \end{Bmatrix} \ , \ A = \begin{bmatrix} \mathbf{0} & \mathbf{I} \\ \mathbf{M}^{-1}\left(\overline{\mathbf{F}}_{(\bar{Y},\bar{Z})(t)} - \mathbf{K}\right) & -\mathbf{M}^{-1}\mathbf{C} \end{bmatrix}, \ B = \begin{bmatrix} \mathbf{0} & \mathbf{0} \\ \mathbf{M}^{-1}\left(\overline{\mathbf{F}}_{(\bar{Y},\bar{Z})(t-\tau)}\right) & \mathbf{0} \end{bmatrix},$$

$$\overline{\mathbf{F}}_{(\bar{Y},\bar{Z})(t)} = \mathbf{Z}\left\{ \sum_{j=0}^{N} -g(\phi)b\mathbf{T}_j^{-1}\begin{pmatrix} K_r \\ K_t \end{pmatrix}\begin{bmatrix} 0 & 1 \end{bmatrix}\mathbf{T}_j \right\},$$

$$\overline{\mathbf{F}}_{(\bar{Y},\bar{Z})(t-\tau)} = \mathbf{Z}\left\{ \sum_{j=0}^{N} g(\phi)b\mathbf{T}_j^{-1}\begin{pmatrix} K_r \\ K_t \end{pmatrix}\begin{bmatrix} 0 & 1 \end{bmatrix}\mathbf{T}_{j-1} \right\}. \tag{21}$$

Assuming the delay period $\tau = n\Delta t$ and Δt is the discrete time interval. The state values $q(t_i - \tau)$ can be calculated by averaging the values at two consecutive sampling intervals as

$$q(t_i - \tau) \approx \frac{q(t_i - \tau + \Delta t) + q(t_i - \tau)}{2} = \frac{q_{i-n+1} + q_{i-n}}{2} \tag{22}$$

Then Eq(20) can be expressed as

$$\dot{q}_i = A_i q_i + \frac{1}{2} B_i \left(q_{i-n+1} + q_{i-n}\right) \tag{23}$$

The differential equation $\dot{q}_i(t)$ has homogenous $q_{Hi}(t)$ and particular $q_{Pi}(t)$ solutions as

$$q_i(t) = q_{Hi}(t) + q_{Pi}(t) \tag{24}$$

where $q_{Hi}(t)$ is obtained as

$$\dot{q}_{Hi}(t) = A_i q_{Hi}(t) \rightarrow q_{Hi}(t) = e^{A_i(t-t_i)}C_0 \tag{25}$$

where C_0 depends on the initial conditions.

$q_{Pi}(t)$ is calculated by

$$q_{Pi}(t) = e^{A_i(t-t_i)}u(t) = -\frac{1}{2}A_i^{-1}B_i\left(q_{i-n+1} + q_{i-n}\right) \tag{26}$$

Then, the complete solution of the differential equation is

$$q_i(t) = e^{A_i(t-t_i)}C_0 - \frac{1}{2}A_i^{-1}B_i(q_{i-n+1} + q_{i-n}) \tag{27}$$

When the state of system is at $t = t_i$

$$q_i = C_0 - \frac{1}{2}A_i^{-1}B_i(q_{i-n+1} + q_{i-n}) \tag{28}$$

C_0 can be obtained from Eq(28)

$$C_0 = q_i + \frac{1}{2}A_i^{-1}B_i(q_{i-n+1} + q_{i-n}) \tag{29}$$

The next state at $t = t_{i+1}$ is as follow

$$q_{i+1} = e^{A_i(t_{i+1}-t_i)}q_i + \frac{1}{2}\left(e^{A_i(t_{i+1}-t_i)} - I\right)A_i^{-1}B_i(q_{i-n+1} + q_{i-n}) \tag{30}$$

The solution requires the previous value q_i and values a delay before q_{i-n+1} and q_{i-n}. The series of equations are expressed at discrete time intervals

$$z_{i+1} = D_i z_i \tag{31}$$

where

$$z_i = \begin{Bmatrix} q_i \\ q_{i-1} \\ q_{i-2} \\ \vdots \\ q_{i-n+1} \\ q_{i-n} \end{Bmatrix}, \quad D_i = \begin{bmatrix} e^{A_i\Delta t} & 0 & \cdots & 0 & \frac{1}{2}\left(e^{A_i\Delta t} - I\right)A_i^{-1} & \frac{1}{2}\left(e^{A_i\Delta t} - I\right)A_i^{-1}B_i \\ I & 0 & \cdots & 0 & 0 & 0 \\ 0 & I & \cdots & 0 & 0 & 0 \\ \vdots & \vdots & \ddots & \vdots & \vdots & \vdots \\ 0 & 0 & \cdots & I & 0 & 0 \\ 0 & 0 & \cdots & 0 & I & 0 \end{bmatrix} \tag{32}$$

Since the milling process is periodic at tooth passing interval, stability of the milling system can be solved by Eq(31) at m number of intervals within the tooth period

$$z_{i+m} = Tz_i = D_m \cdots D_2 D_1 z_i \tag{33}$$

According to Floquet theory, if the eigenvalues of matrix T are less than 1, the system is stable, otherwise the system is unstable. Figure 3 shows the calculation steps of stability lobe diagram by using the semi-discrete time domain method in rotating coordinate frame.
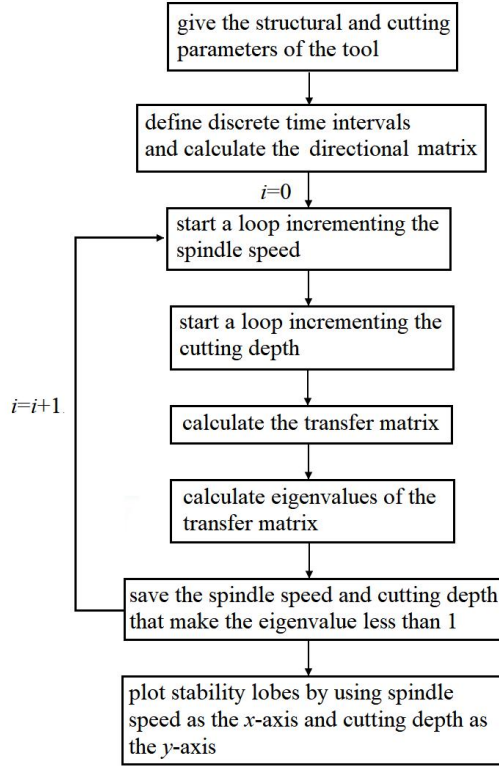
Fig. 3. Calculation steps of stability lobe diagram

3 Numerical Results and Discussion

3.1 Validation

3.1.1 Example 1

Example 1 is to validate the correctness of the semi-discrete time domain solution method used in the model. The milling system model described in rotating coordinate frame is shown in Section 2.2, and the modal parameters of the cutter bar and process parameters are from Ref[23]

$$\omega_{n\bar{Y}} = 2891\,\text{Hz} \quad, \quad \omega_{n\bar{Z}} = 2879\,\text{Hz} \quad, \quad m_{\bar{Y}} = 0.0641\,\text{kg} \quad, \quad m_{\bar{Z}} = 0.0602\,\text{kg} \quad,$$

$$\zeta_{\bar{Y}} = 2.094\% \,, \; \zeta_{\bar{Z}} = 1.779\% \,, \; K_t = 732\,\text{MPa} \,, \; K_r = 56\,\text{MPa} \,, \; N{=}4 \,, \; \phi_{st} = 0° \,, \; \phi_{ex} = 180°$$

Figure 4 shows the chatter stability lobes of milling system in rotating coordinate frame. The present model takes into account the internal damping of the cutter bar, but not that of Ref[23]. Consequently, it can be seen that the position of the lobe diagram calculated by the present model is above the lobe diagram in literature [23]. This shows that the stability of the milling system can be significantly improved if the effect of internal damping is taken into account. If the influence of internal damping is ignored, stability lobes of the present model will be

coincided with the lobes obtained in [23]. The details about expression and solving process of internal damping are shown in literature [21].
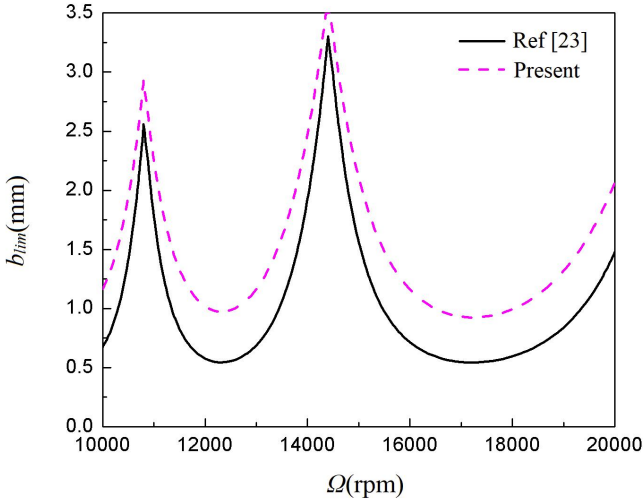

Fig. 4. Chatter stability diagrams in rotating coordinate frame

3.1.2 Example 2

Example 2 is a convergence study of the stability lobes. The geometric parameters of the tapered composite cutter bar are: R_T=0.06m, R_R=0.04m, length l is obtained by the given aspect ratios. Stacking sequence of the composite cutter bar is $\left[\pm\theta\right]_8$. Table 1 gives the material properties of the composite. The process parameters used in the simulation are from Ref[24]:

$$K_t = 1500\text{MPa}, \quad K_r = 450\text{MPa}, \quad N=8, \quad \phi_{st} = 0°, \quad \phi_{ex} = 90°.$$

Table 1. Mechanical properties of carbon/epoxy composite material[25]

ρ(kg/m³)	E_{11}(GPa)	E_{22}(GPa)	G_{12}(GPa)	G_{23}(GPa)	υ_{12}	η_1(%)	η_2(%)	η_4(%)	η_6(%)
1446.2	172.7	7.2	3.76	3.76	0.3	0.45	4.22	7.05	7.05

Results of the convergence study are shown in Table 2 and Figure 5. It can be seen that the convergence result is good with respect to S, and S= 3 is found to be sufficient for convergence. So, all the numerical results of this section are calculated by three mode shape functions.

Table 2. The effect of numbers of mode shape function on $b_{lim,crit}$(non-rotating cutter bar, ζ=0.01, θ=45°, σ=0.75, l/d=10)

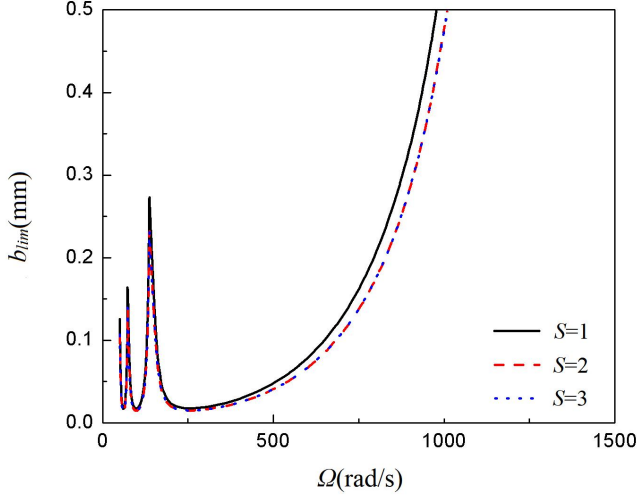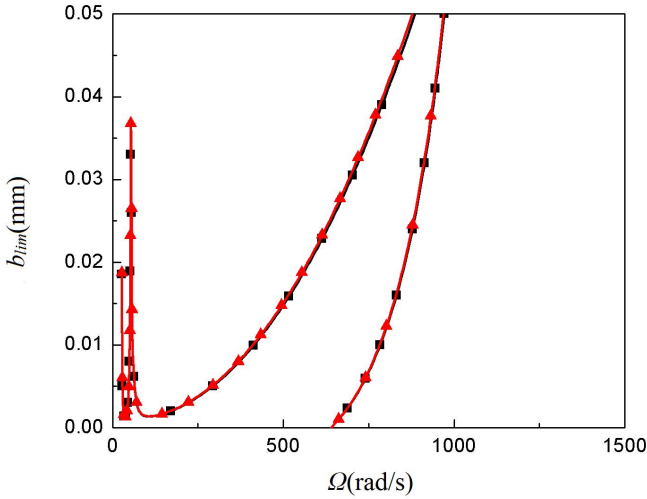| S	1	2	3	4
$b_{lim,crit}$(mm)	0.0166	0.015	0.015	0.015

Fig. 5. Convergences of the stability lobes of the rotating tapered composite cutter bar milling system(ζ=0.01, θ=45°, σ=0.75, l/d=10)

3.1.3 Example 3

Example 3 is the comparison of stability lobes obtained by semi-discrete time domain solution and zero-order approximation frequency domain solution.The involved parameters in simulation are from section 3.1.2. The stacking sequence of the composite cutter bar is [90°]$_6$.

It is seen from figure 6 that the stability lobes solved by the semi-discrete time domain solution are in good agreement with those by the zero-order approximation frequency domain solution.
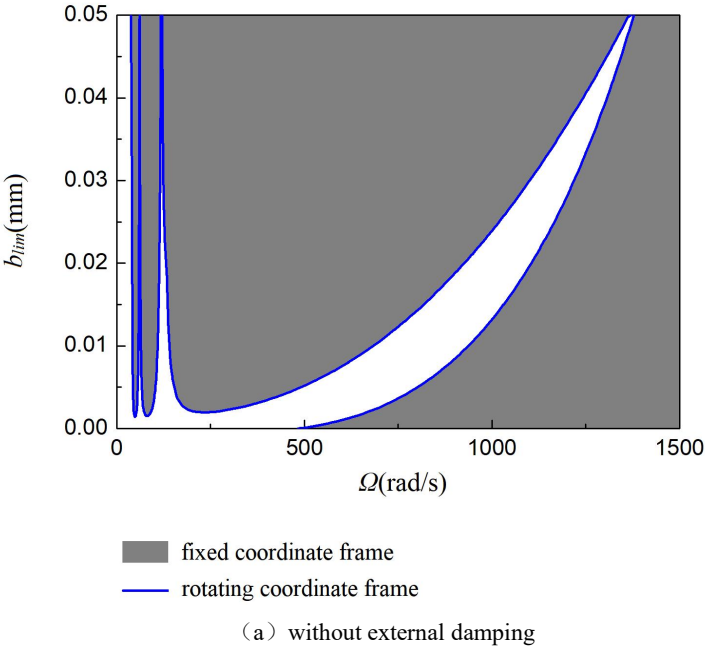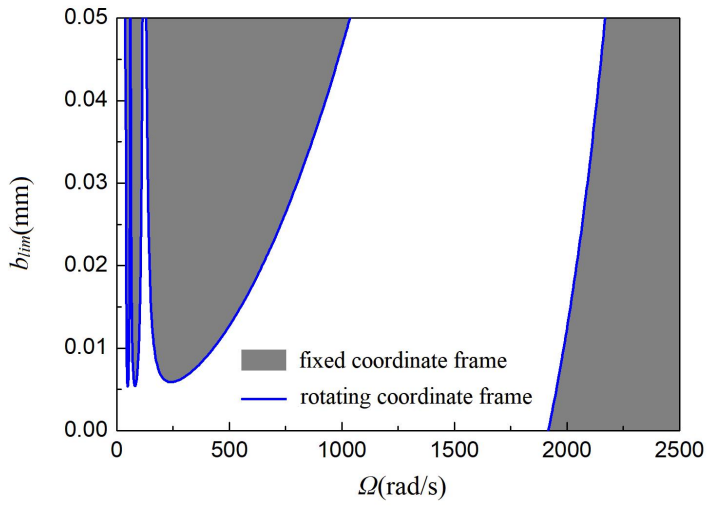
Fig. 6. Zero-order approximation frequency domain method and semi-discrete time domain solution method(ζ=0.01, σ=0.75, l/d=15)

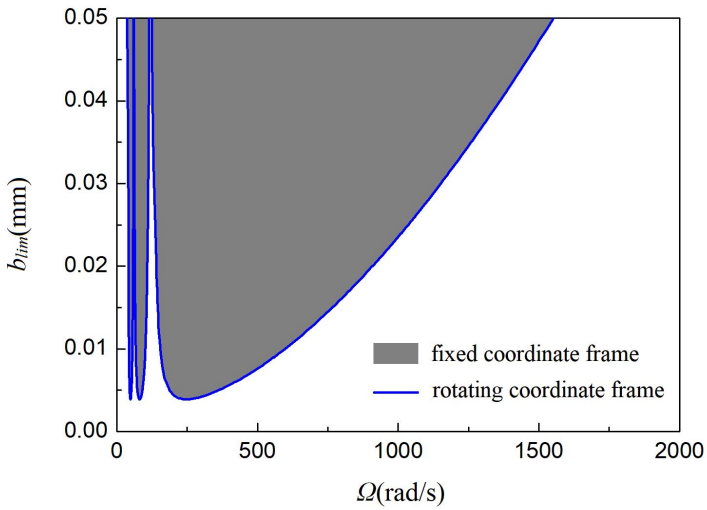## 3.2 Stability Analysis in Rotating and Fixed Coordinate Frame

In this section, the semi-discrete time domain solution method is used to predict the stability of milling system in rotating and fixed coordinate frame. In the following examples, cutting parameters are still from [23].

Figure 7 gives the stability lobes of the milling system which considering the effect of internal and external damping. Figure 7(a), Figure 7(b) and Figure 7(c) show the three cases of without external damping, with internal and external damping and without internal damping. It can be seen that both rotating and fixed coordinate frame give the same results, which indicates that the stability of milling system with an axisymmetric cutter bar are consistent in these two coordinate frames. In addition, it can be seen that no matter whether there is external damping or not, as long as the internal damping is considered, a new unstable region will appear at high rotational speeds.

fixed coordinate frame

rotating coordinate frame

（a）without external damping

（b）with internal and external damping

（c）without internal damping

Fig. 7. Stability lobes of the milling system which considering the effect of internal and external damping
(σ=0.75, θ=90°, l/d=10)

Figure 8 shows the effect of symmetric laminate $[0°]_6$ on the stability of milling system. It can be seen that the lobes obtained in the rotating and fixed coordinate system are coincident no matter at the low rotating speed or at the high rotating speed.

Fig. 8. The effect of symmetric laminate $[0°]_6$ on the stability of milling system (ζ=0.01, σ=0.75, l/d=10)

Figure 9 shows the effect of asymmetric laminate $[90°/45°/-45°/90°/0°_6]$ on the stability of milling system. It can be seen that the lobes obtained in the rotating and fixed coordinate system are coincident no matter at the low rotating speed or at the high rotating speed.
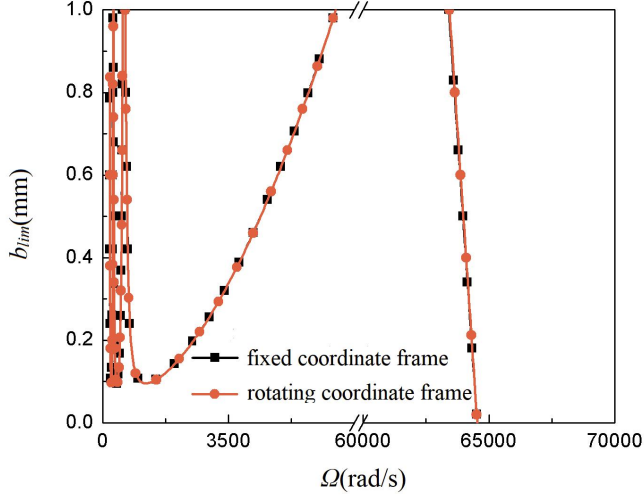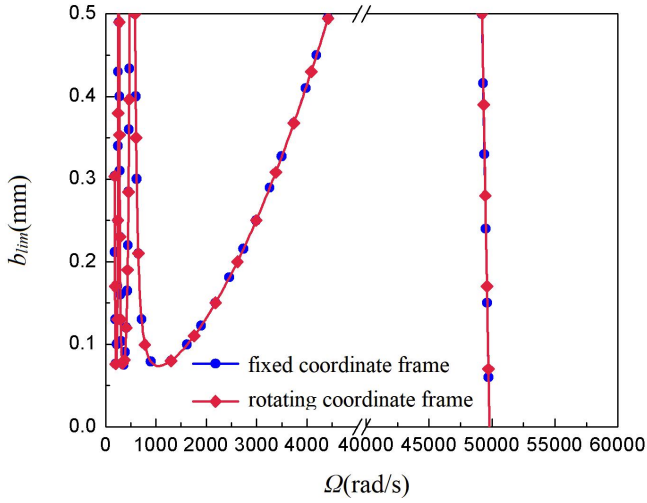

Fig. 9. The effect of asymmetric laminate $[90°/45°/-45°/90°/0°_6]$ on the stability of milling system (ζ=0.01, σ=0.75, l/d=10)

Based on a simple discrete model of 2-DOF cutter bar milling system, literatures [22] and [23] studied the chatter stability of milling system in rotating and fixed frame. The results showed that both rotating and fixed frame give the same results for dynamically symmetric tools (The lumped mass, stiffness and damping parameters are equal in the 2-DOF directions,

respectively). This paper studies the chatter stability of composite cutter bar milling system. The chatter equations are established on a more complex continuous distribution model. It is found that, unlike asymmetrical cutter bar, stability analysis of the milling system with axisymmetric cutter bar remains unchanged no matter how the reference coordinate frame changed. Therefore, compared with literatures [22] and [23], researches in this paper are more general.

4   Conclusions

The chatter stability of milling process in rotating frame is studied in this paper. Cutting force model and structural dynamic equations of composite cutter bar are expressed in rotating coordinate. The chatter equation of tapered composite cutter bar milling system are established in rotating coordinate and discretized by applying Galerkin method. The influences of some factors including internal and external damping, symmetric laminate, and asymmetric laminate on the chatter stability are examined by using the semi-discrete time solution in rotating coordinate frame. Results show that the lobes obtained in the rotating and fixed coordinate system are coincident for dynamically symmetric tools. It is also found that a new chatter instability appears in high-speed regions with the consideration of rotation and internal damping of the composite cutter bar.

Author Contributions

Writing - original draft, Yuhuan Zhang; Methodology, Yongsheng Ren; Formal analysis, Jinfeng Zhang.

References

[1]   L. D. Zhu and C. F. Liu. "Recent progress of chatter prediction, detection and suppression in milling," *Mechanical Systems and Signal Processing*, vol. 143, p. 106840, 2020, https://doi.org/10.1016/j.ymssp.2020.106840.

[2]   D. G. Lee, H. Y. Hwang and J. K. Kim. "Design and manufacture of a carbon fiber epoxy rotating boring bar," *Composite Structures*, vol. 60, no. 1, pp. 115-124, 2003, https://doi.org/10.1016/S0263-8223(02)00287-8.

[3]   S. Nagano, T. Koizumi, T. Fujii, et al. "Development of a composite boring bar," *Composite Structures*, vol. 38, no. 1-4, pp. 531-539, 1997, https://doi.org/10.1016/S0263-8223(97)00089-5.

[4]   J. Wang, F. Wu, Y. L. Han, et al. "Boring bar design with laminar composite structure and research on properties,"(in Chinese), *China Mechanical Engineering*, vol. 24, no. 6, pp. 711-715, 2013, 10.3969/j. issn. 1004-132X. 2013. 06. 001.

[5]   W. Kim, A. Argento and R. A. Scott. "Forced vibration and dynamic stability of a rotating tapered

composite Timoshenko shaft: bending motions in end-milling operations," *Journal of Sound and Vibration*, vol. 246, no. 4, pp. 583-600, 2001, https://doi.org/10.1006/jsvi.2000.3521.

[6] Y. H. Zhang, Y. S. Ren, J. S. Tian, et al. "Chatter stability of the constrained layer damping composite boring bar in cutting process," *Journal of Vibration and Control*, vol. 25, no. 16, pp. 2204-2214, 2019, https://doi.org/10.1177/1077546319852240.

[7] S. Ghorbani, V. A. Rogov, A. Carluccio, et al. "The effect of composite boring bars on vibration in machining process," *The International Journal of Advanced Manufacturing Technology*, vol. 105, no. 1-4, pp. 1157-1174, 2019, https://doi.org/10.1007/s00170-019-04298-6.

[8] J. Tlusty and M. Polacek. "The stability of machine tools against self-excited vibrations in machining," *ASME Int. Res. Prod. Eng.*, vol. 1, no.1, pp. 465-474, 1963.

[9] I. Minis and R. Yanushevsky. "A new theoretical approach for the prediction of machine tool chatter in milling," *Journal of Manufacturing Science and Engineering*, vol. 115, no. 1, pp. 1-8, 1993, https://doi.org/10.1115/1.2901633.

[10] E. Budak and Y. Altintas. "Analytical prediction of chatter stability in milling-part i: general formulation," *Journal of Dynamic Systems, Measurement, and Control*, vol. 120, no. 1, pp. 22-30, 1988, https://doi.org/10.1115/1.2801317.

[11] T. Insperger and G. Stepan. "Updated semi-discretization method for periodic delay-differential equations with discrete delay," *International Journal for Numerical Methods in Engineering*, vol.61, no. 1, pp. 117-141, 2004, https://doi.org/10.1002/nme.1061.

[12] G. Totis. "RCPM - a new method for robust chatter prediction in milling," *International Journal of Machine Tools and Manufacture*, vol. 49, no. 3-4, pp. 273-284, 2009, https://doi.org/10.1016/j.ijmachtools.2008.10.008.

[13] Y. Ding, L. M. Zhu, X. J. Zhang, et al. "A full-discretization method for prediction of milling stability," *International Journal of Machine Tools and Manufacture*, vol. 50, no. 5, pp. 502-509, 2010, https://doi.org/10.1016/j.ijmachtools.2010.01.003.

[14] C. J. Li, A. G. Ulsoy and W. J. Endres. "The effect of flexible-tool rotation on regenerative instability in machining," *Journal of Manufacturing Science and Engineering*, vol. 125, no. 1, pp. 39-47, 2003, https://doi.org/10.1115/1.1536657.

[15] G. L. Xiong, J. M. Yi, C. Zeng, et al. "Study of the gyroscopic effect of the spindle on the stability characteristics of the milling system," *Journal of Materials Processing Technology*, vol. 138, no. 1-3, pp. 379-384, 2003, https://doi.org/10.1016/S0924-0136(03)00102-X.

[16] M. R. Movahhedy and P. Mosaddegh. "Prediction of chatter in high speed milling including gyroscopic effects," *International Journal of Machine Tools and Manufacture*, vol. 46, no. 9, pp. 996-1001, 2006, https://doi.org/10.1016/j.ijmachtools.2005.07.043.

[17] X. Q. Xu, W. X. Tang and S. S. Sun. "Research of gyroscopic effects on the stability of high speed milling," *Key Engineering Materials*, vol. 431-432, pp. 369-372, 2010, https://doi.org/10.4028/www.scientific.net/KEM.431-432.369.

[18] Y. Shi, F. Mahr, U. Wagner, et al. "Gyroscopic and mode interaction effects on micro-end mill dynamics and chatter stability," *International Journal of Advanced Manufacturing Technology*, vol. 65, no. 5-8, pp. 895-907, 2013, https://doi.org/10.1007/s00170-012-4226-9.

[19] B. L. Ma, Y. S. Ren, Y. H. Zhang, et al. "Flutter analysis of milling with consideration of gyroscopic effect," (in Chinese), *Mechanics in Engineering*, vol. 40, no. 4, pp. 372-379, 2018, 10.6052/1000-0879-18-073.

[20] A. Mokhtari, A. Mazidi and M. M. Jalili. "Investigation of rotary inertial dynamic effects on chatter boundary in milling process using three-dimensional Timoshenko tool model," *Proceedings of the Institution of Mechanical Engineers, Part K: Journal of Multi-body Dynamics*, vol. 233, no.1, pp. 93-110, 2019, https://doi.org/10.1177/1464419318788504.

[21] Y. H. Zhang, Y. S. Ren and J. F. Zhang. "Stability analysis of cutting process with internally damped rotating tapered composite cutter bar," *Mathematical Problems in Engineering*, vol.2020, no. 1, pp. 1-23, 2020, https://doi.org/10.1155/2020/2587820.

[22] M. Eynian and Y. Altintas. "Analytical chatter stability of milling with rotating cutter dynamics at process damping speeds," *Journal of Manufacturing Science and Engineering*, vol. 132, no. 2, pp. 021012-1-021012-14, 2010, https://doi.org/10.1115/1.4001251.

[23] A. Comak, O. Ozsahin and Y. Altintas. "Stability of milling operations with asymmetric cutter dynamics in rotating coordinates," *Journal of Manufacturing Science and Engineering*, vol. 138, no. 8, pp. 081004-1-081004-7, 2016, https://doi.org/10.1115/1.4032585.

[24] Y. Altintas and E. Budak. "Analytical prediction of stability lobes in milling," *CIRP Annals-Manufacturing Technology*, vol. 44, no. 1, pp. 357-362, 1995, https://doi.org/10.1016/S0007-8506(07)62342-7.

[25] R. Sino, T. N. Baranger, E. Chatelet, et al. "Dynamic analysis of a rotating composite shaft," *Composites Science and Technology*, vol. 68, no. 2, pp. 337-345, 2008, https://doi.org/10.1016/j.compscitech.2007.06.019.